

Supplementary information

Effects of native defects and Cerium impurity on monoclinic BiVO_4 photocatalyst by PBE+U calculations

Jihua Zhang^{1a*}, Xia Chen^{2a}, MingSen Deng¹, Hujun Shen¹, Hang Li³, Jianwen
Ding^{2*}

¹Guizhou Provincial Key Laboratory of Computational Nano-Material Science,
Guizhou Education University, Guiyang 550018, China

²School of Physics and Optoelectronic Engineering, Xiangtan University, Xiangtan,
411100, China

³Institute for Computational Materials Science, School of Physics and Electronics,
Henan University, Kaifeng 475004, China

E-mail: wuli8@163.com, jwding@xtu.edu.cn

^a These authors contributed equally to this paper.

Table S1 The PBE+U formation energies for the O vacancy defect O_{vac} in the different charge states with the different supercell sizes (96 atoms $2 \times 2 \times 1$ and 192 atoms $2 \times 2 \times 2$ supercells) at the Fermi energy $E_F=0$ under point C conditions.

PBE+U formation energies (eV), $E_F=0$			
Valence state	q=0	q=1	q=2
$2 \times 2 \times 1$	4.76	2.43	0.73
$2 \times 2 \times 2$	4.87	2.59	0.79
ΔH_f	0.11	0.16	0.06

Table S2 Lattice constant of m-BiVO₄ $2 \times 2 \times 1$ supercell for a different type of vacancies at different charged states. Experimental lattice constants (Partially Relaxed method) are included. The result of PBE calculations for Partially Relaxed and Fully Relaxed methods are as listed. The values a, b and c are in Å, the values α , β , and γ are in degrees, and volume is in Å³. The numbers in parentheses are the percent differences (%) of volume between the calculated and the experimental results.

Defect species	Relaxed method	PBE						Volume	
		a	b	c	α	β	γ		
O_{vac} 0	Partially	10.39	10.18	11.70	90.00	90.00	90.39	1236.78 (-)	
	Fully	10.32	10.33	11.76	89.92	89.90	90.02	1253.30 (1.34%)	
+1	Fully	10.23	10.36	11.70	90.15	89.70	90.00	1240.04 (0.26%)	
+2	Fully	10.29	10.28	11.66	90.13	89.82	90.10	1232.93 (-0.31%)	
Bi_{vac} 0	Fully	10.32	10.32	11.70	90.00	90.00	90.01	1246.69 (0.80%)	
	-1	Fully	10.37	10.36	11.80	90.00	90.00	90.00	1267.13 (2.45%)
	-2	Fully	10.41	10.40	11.89	90.00	90.00	89.98	1236.78 (4.12%)
-3	Fully	10.58	10.37	12.24	90.00	90.00	90.23	1343.57 (8.63%)	
V_{vac} 0	Fully	10.36	10.35	11.80	90.00	90.00	90.01	1265.37 (2.31%)	
	-1	Fully	10.41	10.40	11.92	90.00	90.00	90.00	1289.70 (4.28%)
	-2	Fully	10.38	10.53	12.05	90.00	90.00	89.61	1318.23 (6.59%)
	-3	Fully	10.80	10.45	13.19	90.00	90.00	89.85	1488.93 (20.39%)
	-4	Fully	11.27	10.85	14.05	90.00	90.00	93.66	1713.78 (38.57%)
-5	Fully	11.42	11.03	14.11	90.00	90.00	93.96	1773.21 (43.37%)	

Table S3 Using the Partially Relaxed and Fully Relaxed method (PBE or PBE+U), calculated the total energies and 1s core levels of O atom (E_{core}) of m-BiVO₄ for a different type of vacancies at different charged states.

	Relaxed method	PBE		PBE+U	
		Total energy	E_{core}	Total energy	E_{core}
O _{vac} 0	Partially	-703.35	-500.48	-627.20	-500.34
	Fully	-703.51	-500.63	-627.20	-500.34
-1	Partially	-709.44	-500.46	-633.94	-500.32
	Fully	-709.62	-500.52	-634.21	-500.38
-2	Partially	-716.24	-500.52	-639.96	-500.40
	Fully	-716.29	-500.51	-639.99	-500.38
Bi _{vac} 0	Partially	-701.95	-500.86	-625.57	-500.73
	Fully	-702.04	-500.93	-625.74	-500.80
-1	Partially	-698.24	-500.81	-621.73	-500.68
	Fully	-698.55	-501.04	-622.25	-500.92
-2	Partially	-694.50	-500.76	-617.85	-500.64
	Fully	-695.22	-500.76	-618.92	-500.64
-3	Partially	-690.70	-500.71	-613.91	-500.59
	Fully	-692.14	-501.56	-615.84	-501.45
V _{vac} 0	Partially	-688.85	-500.59	-617.20	-500.46
	Fully	-689.11	-500.83	-617.64	-500.70
-1	Partially	-684.83	-500.56	-613.05	-500.42
	Fully	-685.53	-500.97	-614.08	-500.84
-2	Partially	-680.57	-500.59	-608.66	-500.46
	Fully	-681.90	-501.17	-610.45	-501.05
-3	Partially	-676.50	-500.56	-604.47	-500.44
	Fully	-679.09	-502.22	-607.91	-502.08
-4	Partially	-672.40	-500.55	-600.23	-500.43
	Fully	-678.24	-503.33	-608.54	-503.12
-5	Partially	-668.24	-500.53	-595.95	-500.40
	Fully	-677.63	-503.51	-608.48	-503.28

Table S4. Calculated enthalpy of formation per formula unit of m-BiVO₄ and the possible limiting phases by PBE, PBE+U, and HSE06 functional calculation. Experimental values are provided for comparison. (unit: eV)

	PBE	PBE+U	HSE06	Experiment
$\Delta H_f(\text{m-BiVO}_4)$	-11.97	-11.39	-11.96	-12.32 ¹
$\Delta H_f(\text{VO}_2)$	-7.12	-7.73	-7.04	-7.37 ²
$\Delta H_f(\text{V}_2\text{O}_5)$	-16.14	-15.27	-16.54	-16.07 ³
$\Delta H_f(\text{Bi}_2\text{O}_3)$	-6.23	-6.23	-5.82	-5.95 ³
$\Delta H_f(\text{Ce}_2\text{O}_3)$	-11.74	-14.09	-11.03	-18.62 ³
$\Delta H_f(\text{CeO}_2)$	-10.45	-10.44	-11.02	-11.28 ³

Table S5 Experimental lattice constants used for the PBE, PBE+U, and HSE06 functional total energy calculations. The values a, b and c are in Å, and the values α , β and γ are in degrees

	K-Points	Space group	Experiment
VO ₂	8×8×12	P4 ₂ /mnm	a=b=4.5561, c=2.8598; $\alpha=\beta=\gamma = 90^\circ$ ⁴
V ₂ O ₅	3×8×10	Pmn21	a=11.48, b=4.360, c=3.555; $\alpha=\beta=\gamma = 90^\circ$ ⁵
Bi ₂ O ₃	6×4×5	P12 ₁ /c1	a=5.8444, b=8.1574, c=7.5032; $\alpha=90^\circ$, $\beta=112.97^\circ$, $\gamma=90^\circ$ ⁶
Ce ₂ O ₃	10×10×5	P321	a=b=3.888, c=6.07 $\alpha=\beta=90^\circ$, $\gamma = 120^\circ$ ⁷
CeO ₂	6×6×6	FM3-M	a=b=c=5.411; $\alpha=\beta=\gamma = 90^\circ$ ⁸

Table S6. The PBE, PBE + U, and HSE06 functional calculated chemical potentials at the representative chemical potential limits imposed by the formation of competing for binary oxides for m-BiVO₄, as indicated in Fig. S1 and Fig. 1, respectively. All energies are given in eV.

PBE					PBE+U				
	A	D	E'	F	M'	C	E	O	M
μ_{Bi}	-7.77	-3.87	-6.99	-3.87	-6.87	-7.53	-6.99	-5.35	-6.87
μ_{V}	-17.06	-11.26	-17.84	-12.64	-15.99	-12.55	-13.09	-10.37	-12.32
μ_{O}	-4.93	-7.36	-4.93	-7.01	-5.42	-4.93	-4.93	-6.02	-5.16
μ_{Ce}	-16.37	-11.51	-16.37	-12.21	-15.39	-14.46	-14.46	-12.28	-14.23
HSE06									
	A _{HSE}	D _{HSE}	E _{HSE}	F _{HSE}	M _{HSE}				
μ_{Bi}	-8.05	-4.36	-4.36	-7.27	-6.36				
μ_{V}	-18.54	-12.39	-14.47	-19.32	-16.27				
μ_{O}	-6.36	-8.82	-8.3	-6.36	-7.35				
μ_{Ce}	-17.62	-12.7	-13.74	-17.62	-15.64				

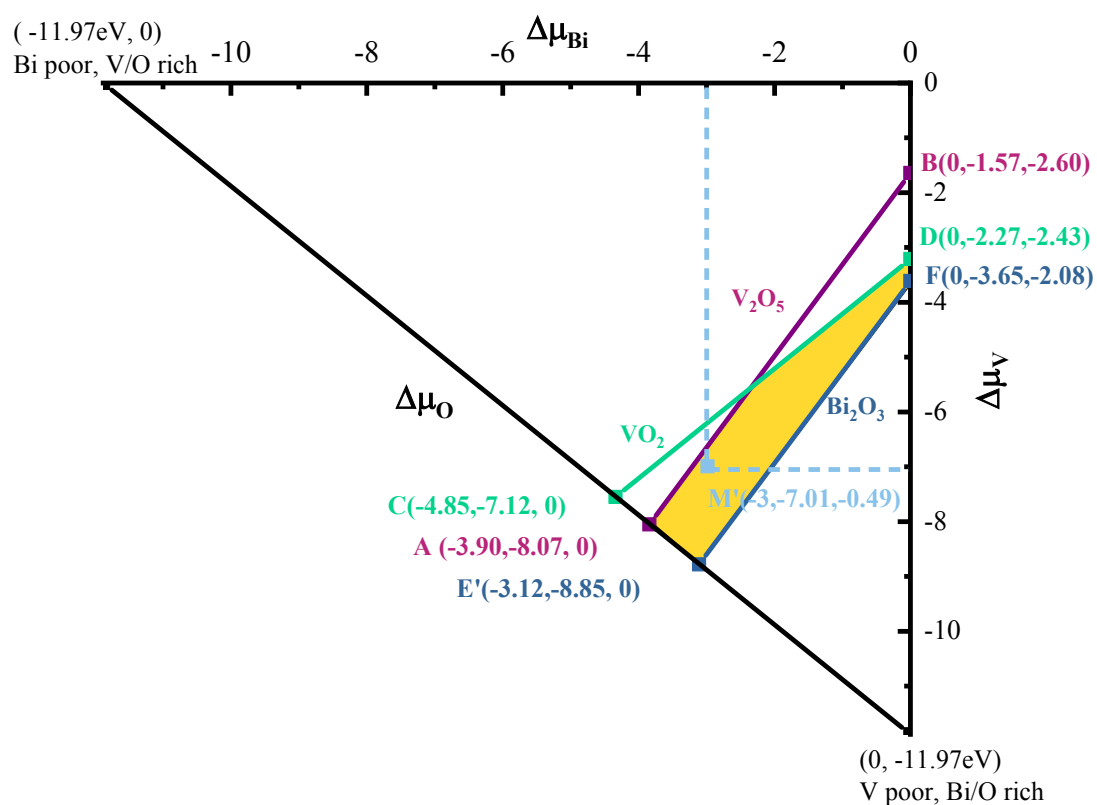


Fig. S1 Accessible range of chemical potentials (yellow/shaded region) for the equilibrium growth condition of $m\text{-BiVO}_4$, which calculate by PBE. Specific points A, D, E', F, and M' are chosen as the representative chemical potentials for the following defect formation energy.

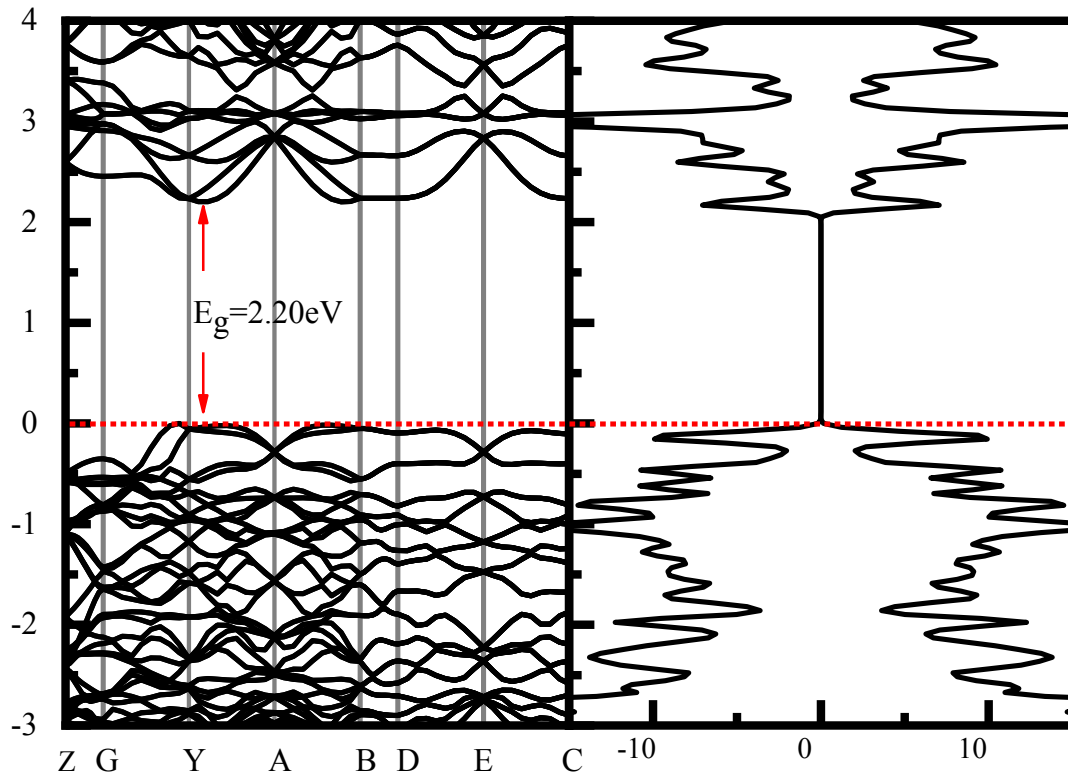


Fig. S2 The band structures and total density of state calculated for ideal m-BiVO₄ by PBE functional. The position of the VBM is placed at zero for easy comparison.

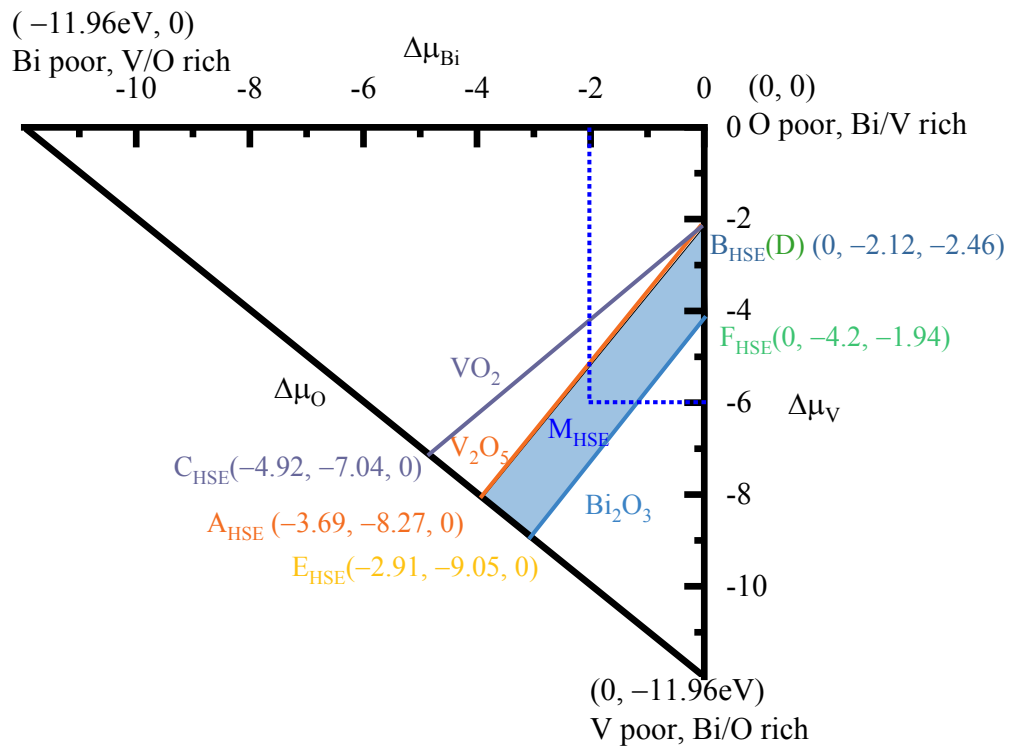


Fig. S3 Accessible range of chemical potentials (light blue /shaded region) for the equilibrium growth condition of m-BiVO₄, which calculate by HSE06 functional. Specific points A_{HSE}, D_{HSE}, E_{HSE}, F_{HSE}, and M_{HSE} are chosen as the representative chemical potentials for the following defect formation energy.

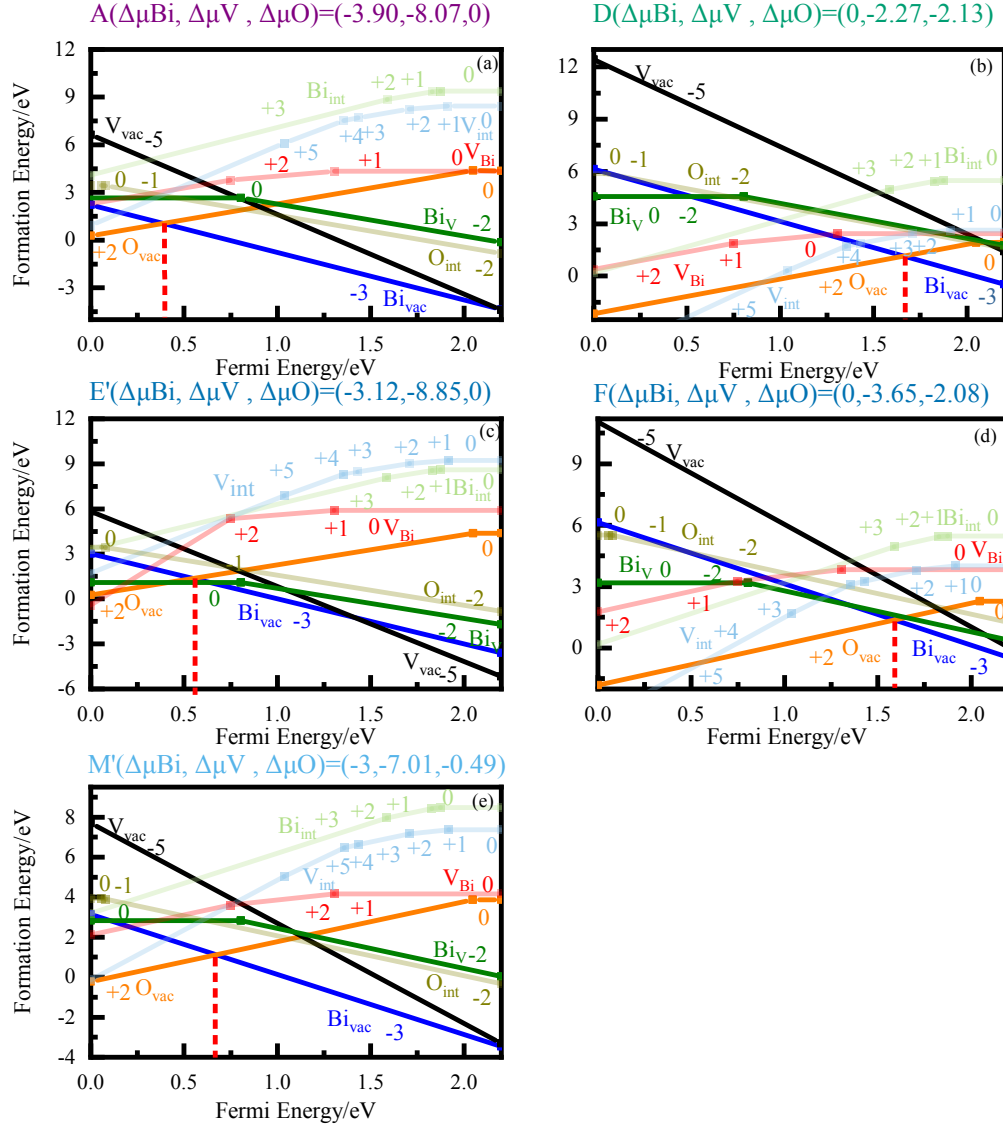


Fig. S4 The formation energies (derived from PBE calculated total energies of supercells) of intrinsic defects Bi_{vac} , V_{vac} , O_{vac} , Bi_{v} , V_{Bi} , O_{int} , Bi_{int} , and V_{int} in $m\text{-BiVO}_4$ at different chemical conditions A, D, E', F, and M' (in fig. S1), plotted as a function of the Fermi level concerning the VBM. The Fermi-level pinnings are indicated by red dashed lines. The Fermi level (EF) at the valence band maximum (VBM) and the conduction band minimum (CBM) is set to 0.00 and 2.20 eV, respectively. The numbers in the plot indicate the defect charge state; parallel lines imply equal charge states. For each geometrical defect, only the charge states that are energetically most favorable at a given Fermi energy are shown.

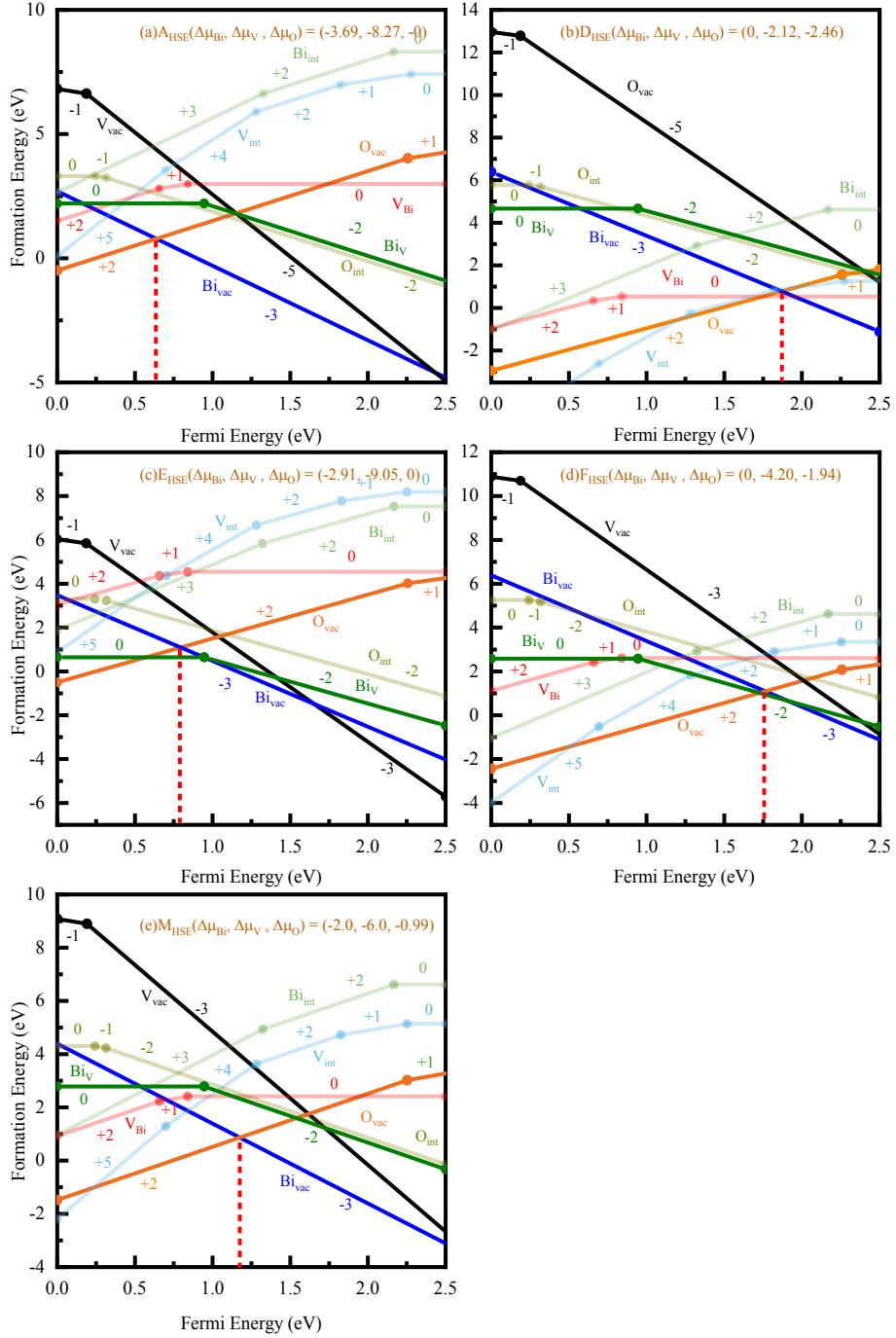


Fig. S5 The formation energies (derived from HSE06 functional calculated total energies of supercells) of intrinsic defects Bi_{vac} , V_{vac} , O_{vac} , Bi_{v} , V_{bi} , O_{int} , Bi_{int} , and V_{int} in $m\text{-BiVO}_4$ at different chemical conditions A_{HSE} , D_{HSE} , E_{HSE} , F_{HSE} , and M_{HSE} (in fig. S3), plotted as a function of the Fermi level with respect to the VBM. The Fermi-level pinnings are indicated by red dashed lines. The Fermi level (EF) at the valence band maximum (VBM) and the conduction band minimum (CBM) is set to 0.00 and 2.50 eV, respectively. The numbers in the plot indicate the defect charge state; parallel lines imply equal charge states. For each geometrical defect, only the charge states that are energetically most favorable at a given Fermi energy are shown.

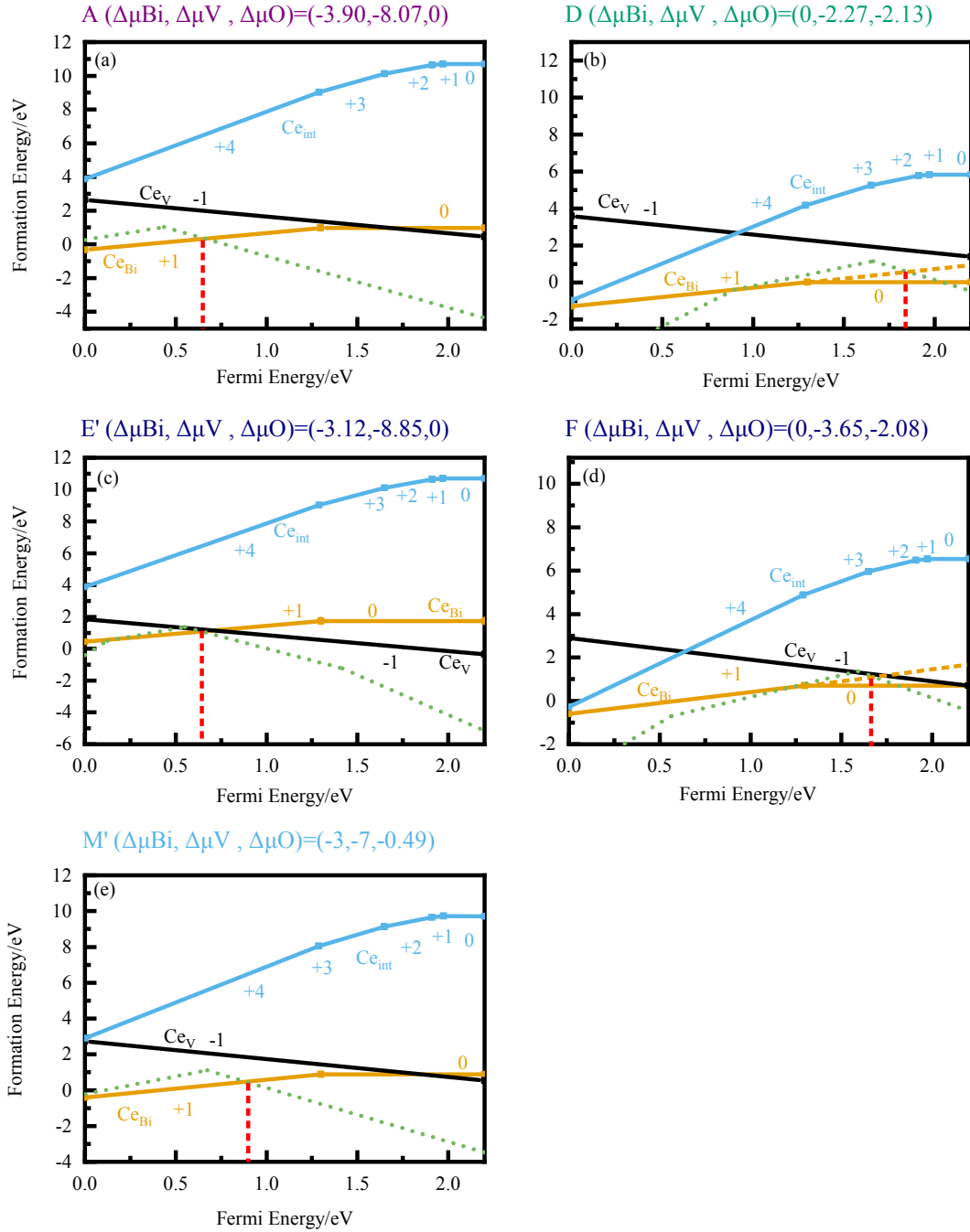


Fig. S6 The PBE calculated results for the formation energies of Ce doping in m-BiVO₄ using chemical potentials corresponding to points A, D, E', F, and M' in Fig. S1. The energetic value of the Fermi level pinning is indicated by red dashed lines. The E_{F} at the VBM and the CBM is set to 0.00 and 2.20 eV, respectively. The numbers in the plot indicate the defect charge state; parallel lines imply equal charge states. For each defect, only the charge states that are energetically most favorable at a given Fermi energy are shown.

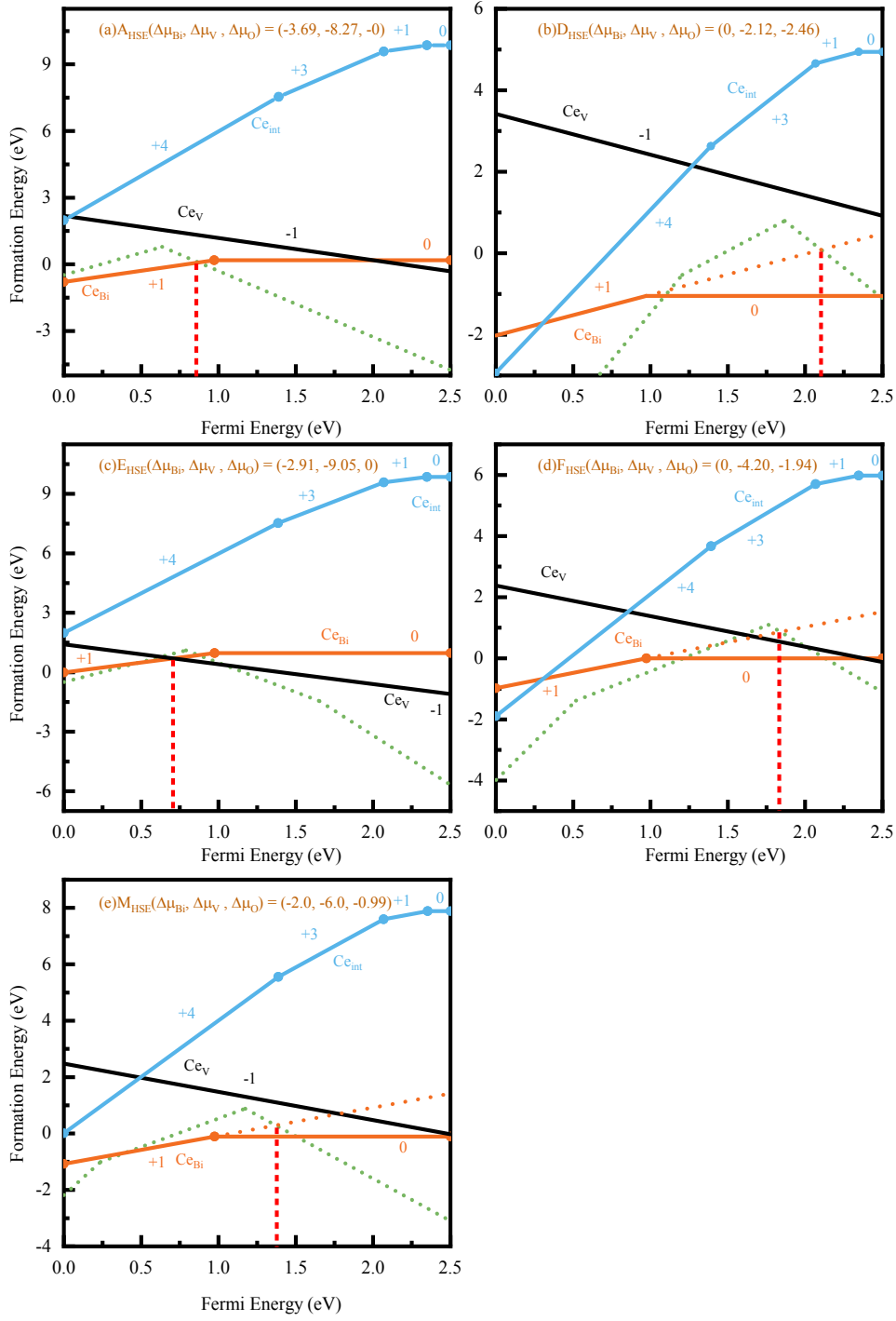


Fig. S7 The HSE06 functional calculated formation energies of Ce doping in m-BiVO₄ using chemical potentials corresponding to A_{HSE} , D_{HSE} , E_{HSE} , F_{HSE} , and M_{HSE} (in fig. S3). The energetic value of the Fermi Level Pinning is indicated by red dashed lines. The E_{F} at the VBM and the CBM is set to 0.00 and 2.50 eV, respectively. The numbers in the plot indicate the defect charge state; parallel lines imply equal charge states. For each defect, only the charge states that are energetically most favorable at a given Fermi energy are shown.

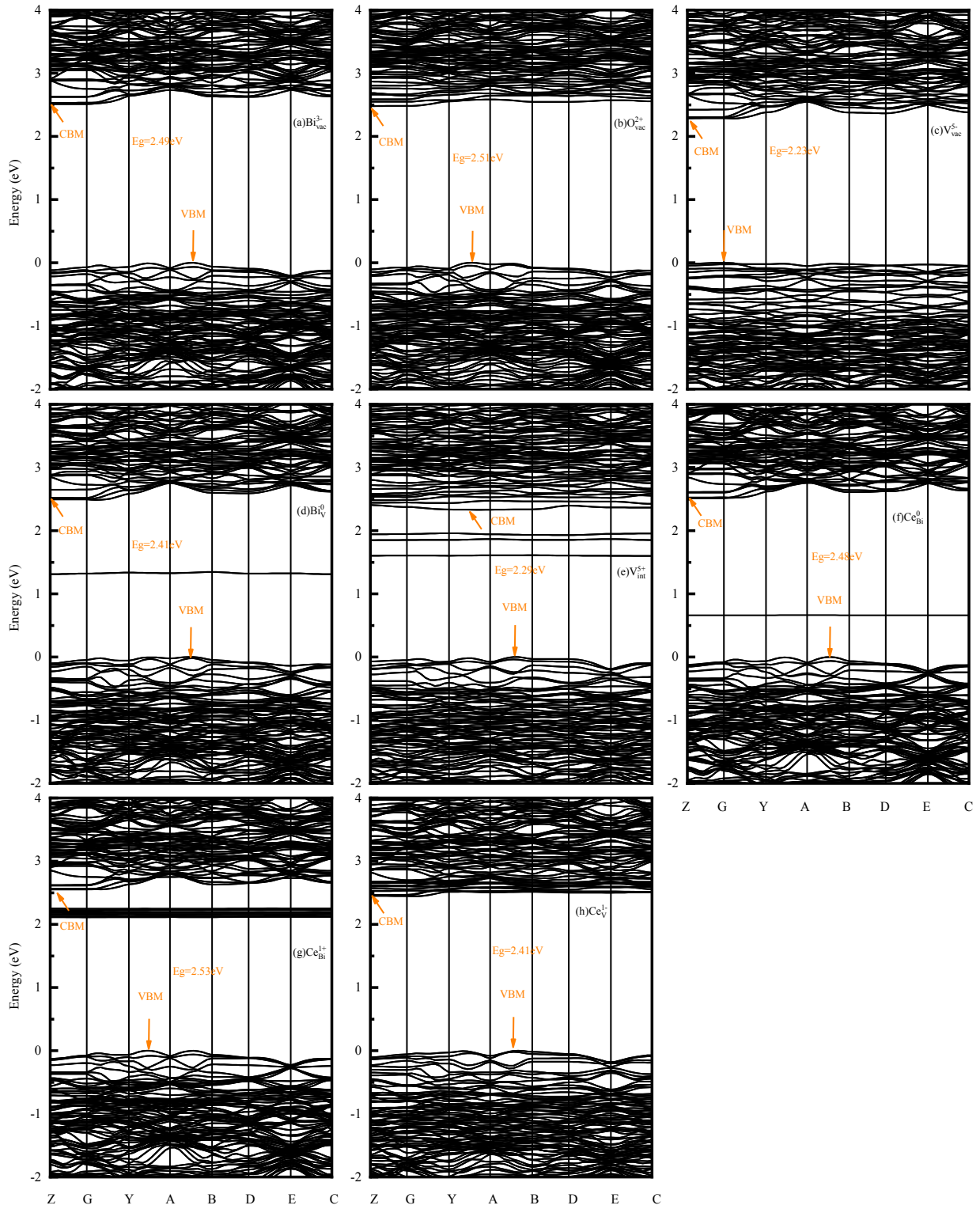


Fig. S8 The PBE+U calculated band structure of (a) $\text{Bi}_{\text{vac}}^{3-}$, (b) $\text{O}_{\text{vac}}^{2+}$, (c) $\text{V}_{\text{vac}}^{5-}$, (d) Bi_{V}^0 , (e) $\text{V}_{\text{int}}^{5+}$, (f) Ce_{Bi}^0 , (g) $\text{Ce}_{\text{Bi}}^{1+}$, and (h) $\text{Ce}_{\text{V}}^{1-}$ defects. The position of the VBM is placed at zero for easy comparison.

Reference

1. A. W. Sleight, H. y. Chen, A. Ferretti and D. E. Cox, *Mater. Res. Bull.*, 1979, 14, 1571-1581.
2. M. Matsubara, R. Saniz, B. Partoens and D. Lamoen, *Phys. Chem. Chem. Phys.*, 2017, 19, 1945-1952.
3. W. M. Haynes, D. R. Lide and T. J. Bruno, *CRC handbook of chemistry and physics*, CRC Press, Boca Raton, Florida, 2014.
4. D. B. McWhan, M. Marezio, J. P. Remeika and P. D. Dernier, *Phys. Rev. B*, 1974, 10, 490-495.
5. J. A. A. Ketelaar, *Nature*, 1936, 137, 316-316.
6. S. A. Ivanov, R. Tellgren, H. Rundlöf and V. G. Orlov, *Powder Diffr.*, 2001, 16, 227-230.
7. W. Zachariasen, *Z. Phys. Chem.*, 1926, 123, 134-150.
8. M. G. Harwood, *Nature*, 1949, 164, 787-787.